Biomedicine & Pharmacotherapy 171 (2024) 116124

Contents lists available at ScienceDirect

Biomedicine & Pharmacotherapy

journal homepage: www.elsevier.com/locate/biopha

Therapeutic strategy using novel RET/YES1 dual-target inhibitor in lung cancer

Yong June Choi [a], Munkyung Choi [a], Jaewoo Park [a], Miso Park [a,b], Myung Jun Kim [a], Jae-sun Lee [c], Su-jin Oh [c], Young Joo Lee [a], Wan Seob Shim [a], Ji Won Kim [d], Myung Jin Kim [c], Yong-Chul Kim [c,e], Keon Wook Kang [a,*]

[a] College of Pharmacy and Research Institute of Pharmaceutical Sciences, Seoul National University, Seoul 08826, Republic of Korea
[b] Department of Pharmacy, Kangwon National University, Chuncheon 24341, Republic of Korea
[c] R&D Center, PeLeMed, Co. Ltd., Seoul 06100, Republic of Korea
[d] Jeju Research Institute of Pharmaceutical Sciences, College of Pharmacy, Jeju National University, Jeju 63243, Republic of Korea
[e] School of Life Sciences, Gwangju Institute of Science and Technology, Gwangju 61005, Republic of Korea

ARTICLE INFO

Keywords:
Lung cancer
Metastasis
CCDC6-RET
YES1-Cortactin-actin remodeling pathway
RET/YES1 dual-target inhibitor

Chemical compounds studied in this article:
PLM-101 (no PubChem CID)
Dasatinib (PubChem CID: 3062316)
Osimertinib (PubChem CID: 71496458)

ABSTRACT

Lung cancer represents a significant global health concern and stands as the leading cause of cancer-related mortality worldwide. The identification of specific genomic alterations such as *EGFR* and *KRAS* in lung cancer has paved the way for the development of targeted therapies. While targeted therapies for lung cancer exhibiting *EGFR*, *MET* and *ALK* mutations have been well-established, the options for *RET* mutations remain limited. Importantly, *RET* mutations have been found to be mutually exclusive from other genomic mutations and to be related with high incidences of brain metastasis. Given these facts, it is imperative to explore the development of RET-targeting therapies and to elucidate the mechanisms underlying metastasis in RET-expressing lung cancer cells. In this study, we investigated PLM-101, a novel dual-target inhibitor of RET/YES1, which exhibits notable anti-cancer activities against CCDC6-RET-positive cancer cells and anti-metastatic effects against YES1-positive cancer cells. Our findings shed light on the significance of the YES1-Cortactin-actin remodeling pathway in the metastasis of lung cancer cells, establishing YES1 as a promising target for suppression of metastasis. This paper unveils a novel inhibitor that effectively targets both RET and YES1, thereby demonstrating its potential to impede the growth and metastasis of RET rearrangement lung cancer.

1. Introduction

Lung cancer is the leading cause of cancer-related mortality globally [1,2], with 5-year survival rates ranging from 4 to 17 % depending on stage and regional variations [3]. The annual incidence of newly diagnosed lung cancer cases is estimated to be 1.8 million, resulting in 1.6 million deaths [4,5]. Extensive research in recent decades has focused on unraveling the molecular mechanisms underlying development of lung cancer [6,7]. Consequently, various genomic alterations including *EGFR*, *KRAS*, *BRAF*, *MET*, *ALK*, *ROS1*, and *RET* have been identified as oncogenic drivers in lung cancer [7–9]. Precise targeted therapies based on the specific mutation present in each lung cancer patient are crucial, since lung cancer cells proliferate in response to overactivation of mutant proteins [10].

Rearranged during transfection (*RET*) is a proto-oncogene encoding a receptor tyrosine kinase, and is associated with the proliferation and survival of several types of cancer [11,12]. Genomic alterations in *RET* are found in ~2 % of non-small cell lung cancer (NSCLC) cases and ~20 % of papillary thyroid carcinoma (PTC) cases [11]. The most common forms of *RET* rearrangements are CCDC6-RET and KIF5B-RET, which

Abbreviations: ARK5, AMPK-related protein kinase 5; EMT, epithelial-mesenchymal transition; ERK, extracellular signal-regulated kinase; FBS, fetal bovine serum; FDA, Food and Drug Administration; ICI, immune checkpoint inhibitor; MAPK, mitogen-activated protein kinase; MEK, mitogen-activated protein kinase kinase; mTOR, mammalian target of rapamycin; MMP, matrix metalloproteinase; NCBI, National Center for Biotechnology Information; NSCLC, non-small cell lung cancer; NSGA, NOD/ShiLtJ-*Prkdc*^{em1AMC}*Il2rg*^{em1AMC}; ORR, objective response rate; PI3K, phosphoinositide 3-kinase; P/S, penicillin/streptomycin; PTC, papillary thyroid cancer; RET, rearranged during transfection; TMB, tumor mutational burden; WASP, Wiskott–Aldrich syndrome protein.

* Corresponding author.
E-mail address: kwkang@snu.ac.kr (K.W. Kang).

https://doi.org/10.1016/j.biopha.2024.116124
Received 4 August 2023; Received in revised form 20 December 2023; Accepted 2 January 2024
Available online 9 January 2024

aberrantly activate RET kinase and downstream signaling pathways such as RAS/mitogen-activated protein kinase (MAPK) and phosphoinositide 3-kinase (PI3K)/AKT [13]. While targeted therapies against mutations in *EGFR*, *MET*, *ALK*, and *ROS1* are well-established, options for RET-targeted therapies remain limited [14]. Importantly, *RET* genomic alterations are thought to be mutually exclusive from other genomic mutations such as *EGFR*, *KRAS*, *BRAF*, and *ALK* [15], emphasizing the need for the development of RET-specific therapeutic strategies.

Metastasis, the dissemination of primary cancer to distant organs, is a major contributor to cancer-related mortality [16,17]. Lung cancer is especially renowned for its ability to spread rapidly, as well as its potency to disseminate to various organs with distinct anatomical and physiological characteristics [18]. Approximately 50 % of lung cancer patients are diagnosed with metastatic cancers [19]. NSCLC commonly metastasizes to sites such as the brain (47 %), bone (36 %), liver (22 %), adrenal glands (15 %), thoracic cavity (11 %), and distant lymph nodes (10 %) [20]. Late-stage lung cancer patients with numerous metastases pose significant challenges in terms of treatment [21,22]. Of note, a recent study has shown that patients who have abnormalities in the *RET* gene exhibit particularly high incidences of brain metastasis [23]. Despite its significance, the specific molecular and cellular mechanisms underlying metastasis in lung cancer remain poorly understood [24,25]. Thus, it is crucial to elucidate the mechanisms contributing to lung cancer metastasis and to develop efficient strategies to target them.

Cancer cell metastasis is a complex process involving a series of integrated steps, beginning with membrane extension and protrusion [26]. Actin polymerization during metastasis can be viewed as the "feet" of cancer cells. Mechanisms regulating actin remodeling in cancer cells, including the Wiskott–Aldrich syndrome protein (WASP)/Arp2/3 complex, LIM-kinase/Cofilin, and Cortactin pathways, have been extensively investigated due to their significance in cancer cell migration and invasion [27–30]. Therefore, targeting of the mechanisms of actin remodeling pathway could be an effective approach to suppression of the “feet” of cancer cells and prevention of metastasis thereby.

YES1, one of the eight members of the SRC family kinases [31], is recognized as a non-receptor tyrosine kinase residing in the cytosol. SRC family kinases interact with various other kinases to regulate the growth and metastasis of cancer [32,33]. Previous studies have indicated that RET plays a role in regulating SRC activity [34], and that SRC, in turn, regulates actin polymerization through Cortactin activity [35,36]. Furthermore, a study has demonstrated that one of the RET rearrangements, KIF5B-RET, regulates invadopodia formation in cancer cells through SRC activation [37]. However, there is currently insufficient research on the involvement of YES1 in the RET or actin polymerization pathway.

In this study, we investigated PLM-101, a novel dual-target inhibitor that simultaneously targets RET and YES1. Our findings show that PLM-101 exhibits anti-cancer activity in CCDC6-RET-positive NSCLC/PTC cancer cells. Notably, PLM-101 effectively reduced the tumor volume in an animal model of CCDC6-RET-positive cancer. Additionally, we have confirmed that inhibiting the YES1-Cortactin-actin remodeling pathway suppresses the invasion of metastatic lung cancer cells. Moreover, in animal models into which metastatic lung cancer cells were injected via the tail vein, PLM-101 effectively blocked metastasis. These findings highlight a possible link between the YES1-Cortactin-actin remodeling pathway and the metastasis of lung cancer. To the best of our knowledge, this study is the first to elucidate the involvement of YES1 in both the activation pathway of RET and the actin remodeling pathway. In this paper then, we introduce a novel RET/YES1 dual-target inhibitor as a promising therapeutic strategy for inhibition of lung cancer growth and metastasis.

2. Materials and methods

2.1. Cell lines

Human lung cancer cell lines HCC827, PC9, A549, H1993, and H292 were cultured in RPMI 1640 medium supplemented with 10 % fetal bovine serum (FBS, #16000–044, ThermoFisher, Waltham, MA, USA) and 1 % penicillin/streptomycin solution (P/S, #SV30010, Hyclone, Logan, UT, USA), while the LC2/ad cell line was cultured in HamF12: RPMI1640 (1:1) medium supplemented with 15 % FBS, 1 % P/S, and 25 mM HEPES. The human thyroid cancer cell lines TPC1 and 8505 C, as well as the human embryonic kidney cell line HEK293T, were cultured in DMEM high glucose medium supplemented with 10 % FBS and 1 % P/S. The Ba/F3 cell line was maintained in RPMI 1640 medium supplemented with 5 % FBS and 1 % P/S along with 10 ng/ml of mouse IL-3. In the case of the specific kinase overexpressing Ba/F3 cells, cells were maintained in 10 % FBS and 1 % P/S without mouse IL-3. All cell lines were cultured in a humidified incubator at 37 ℃ with 5 % CO_2.

2.2. Chemicals and antibodies

The PLM-101 compound was donated from PeleMed (Seoul, South Korea). Dasatinib (#HY-10181), Osimertinib (#HY-15772) were purchased from MedChemExpress (Monmouth Junction, NJ, USA). Primary antibodies against RET (#3220 S), phospho-RET Tyr905 (#3221 S), PARP/cleaved-PARP (#9532 S), Caspase-3 (#9662 S), cleaved-Caspase-3 (#9664 S), Cyclin D1 (#2978 S), AKT (#9272 S), phospho-AKT ser473 (#9271 S), p70S6K (#9202 S), phospho-p70S6K Thr389 (#9234 S), MEK1/2 (#8727 S), phospho-MEK1/2 Ser217/221 (#9154 S), ERK1/2 (#9102 S), phospho-ERK1/2 Thr202/tyr204 (#9101 S), mTOR (#2972 S), phospho-mTOR Ser2448 (#2971), ARK5 (#4458 S), YES1 (#3201 S), SRC (#2108 S), phospho-SRC family Tyr416 (#2101 S), and Cortactin (#3502 S) were purchased from Cell Signaling Technology (Danvers, MA, USA). Primary antibodies against phospho-RET Tyr1015 (#PA5–105930), p90RSK1/2/3 (#PA5–17680), and phospho-p90RSK1 Ser380 (#PA5–17900) were purchased from Invitrogen (Waltham, MA, USA). Primary antibodies against glyceraldehyde 3-phoshate dehydrogenase (GAPDH) (#CB1001) and phospho-Cortactin Tyr421 were purchased from Merck Millipore (Burlington, MA, USA). Primary antibodies against beta-actin (#A2228) was purchased from Sigma-Aldrich (St. Louis, MO, USA). Primary antibodies against Cyclin B1 (#sc-245), Cyclin E (#sc-377100), matrix metalloproteinase (MMP)–2 (#sc-10736), and MMP-9 (#sc-10737) were purchased from Santa Cruz Biotechnology (Dallas, TX, USA). Primary antibodies against E-cadherin (#610181) and N-cadherin (#610920) were purchased from BD Biosciences (Franklin Lakes, NJ, USA). Horseradish peroxidase (HRP)-linked secondary antibodies against anti-rabbit IgG (#7074 S) and anti-mouse IgG (#7076 S) were purchased from Cell Signaling Technology (Danvers, MA, USA). IVISbrite D-luciferin potassium salt (#122799, PerkinElmer, Waltham, MA, USA) was used to measure *in vivo* luminescence.

2.3. In vitro kinase activity assay

The *in vitro* kinase activity was measured using the HTRF KinEASE-TK kit (Cisbio, Codolet, France) as described in previous studies [38]. In brief, a reaction was performed using 1 ng of kinase enzyme, 100 μM ATP, and 0.1 μM kinase substrate, along with serially diluted inhibitor in a kinase reaction buffer (containing 50 mM HEPES, pH 7.0, 0.1 mM orthovanadate, 5 mM MgCl2, 1 mM DTT, 0.01 % BSA, and 0.02 % NaN3). The time-resolved fluorescence energy transfer (TR-FRET) signal was detected by Victor multi-label reader (Perkin Elmer). The IC_{50} values were calculated using GraphPad Prism 7.0 (GraphPad Software Inc, San Diego, CA, USA).

2.4. Ba/F3 proliferation assay

Ba/F3 cells overexpressing the RET mutant kinase were seeded in 96-well plates (3×10^3 cells/well, 90 μL) and serially diluted PLM-101 was added to each well (10 μL each). After 72 h incubation, cell viability was measured using CellTiter-Glo (#G7573, Promega, Madison, WI, USA). The GI_{50} values were calculated using GraphPad Prism 7.0.

2.5. Cell proliferation assay

The IncuCyte Zoom/IncuCyte S3 Live Cell Analysis System (Sartorius, Gottingen, Germany) were used to conduct cancer cell proliferation assay lasting less than 4 days. Cancer cells were seeded in 96-well plate (2×10^3 cells/well), and after the drug treatment, cell confluence was scanned and analyzed by IncuCyte Zoom/IncuCyte S3 Live Cell Analysis System.

2.6. Colony formation assay

To evaluate the ability of PLM-101 to inhibit colony formation on cancer cells, various cancer cells were seeded at very low density in 6-well plate (2×10^3 cells/well). The drug-containing medium was replaced every 72 h and the experiment was terminated when the cell confluence in the untreated group reached 90–95 %. The wells were washed with cold PBS, and 1 ml of crystal violet solution (#V5256, Sigma-Aldrich) was added for cell staining. The stained cells were fixed with 4 % paraformaldehyde and photographically documented. The crystal violet positive area was analyzed using imageJ software (Rasband, W.S., ImageJ, U. S. National Institutes of Health, Bethesda, Maryland, USA).

2.7. Apoptosis and cell cycle analyses by flow cytometry

After 24 h drug incubation, the cells were detached and incubated in 70 % ethanol in PBS at –20 ℃ for 24 h for fixation. After fixation, cells were stained in the staining buffer containing 0.2 % propidium iodide solution (#P4864, Sigma-Aldrich), 0.1 % RNase A solution (#12091–039, Invitrogen), and 0.1 % triton-X100 (#T8532, Sigma-Aldrich) for 30 min at room temperature in the dark. The DNA contents in the cancer cells were measured by flow cytometry (Novocyte, Agilent, Santa Clara, CA, USA).

2.8. Immunoblotting

Cells were lysed in a lysis buffer (10 mM Tris-Cl, 1 % triton X-100, 100 mM sodium chloride, 10 % glycerol, 1 mM EDTA, 30 mM sodium pyrophosphate, 5 mM glycerol-2-phophate, 1 mM sodium fluoride, 1 mM sodium orthovanadate, 1 % phosphatase inhibitor cocktail 2 (#P5726, Sigma-Aldrich), 1 % phosphatase inhibitor cocktail 3 (#P0044, Sigma-Aldrich), and 0.02 tablet/ml protease inhibitor cocktail (#11697498001, Roche, Basel, Switzerland). The protein concentrations of samples were quantified by the bradford assay. Prepared protein samples were separated on SDS-polyacrylamide gels and transferred to 0.45 μm nitrocellulose membranes (#10600002, Cytiva, Marlborough, MA, USA). The membranes were blocked with 5 % skim milk in PBST (phosphate-buffered saline with 0.1 % tween 20). The primary antibodies were incubated overnight at 4 ℃, and the secondary antibodies were incubated 1 h at room temperature. The membranes were visualized using a chemiluminescent HRP substrate (#WBKLS0500, Merck Millipore, Burlington, MA, USA) and detected by LAS-3000 mini (Fujifilm, Tokyo, Japan). All western blot results were replicated independently for a minimum of three times. The CCDC6-RET protein was detected using the RET antibody (#3220 S, Cell Signaling Technology).

2.9. Small interfering RNA (siRNA) transfection

The knockdown of *CCDC6-RET*, *YES1, and ARK5* was achieved using Lipofectamine 2000 transfection reagents (#11668027, ThermoFisher) according to the manufacturer's instructions. Briefly, to start the transfection process, Lipofectamine 2000 and TOM media (transfection optimized medium, #TR 004–01, WELGENE, Gyeongsan, South Korea) were mixed and incubated for 5 min. Subsequently siRNA was added to the mixture and incubated for an additional 20 min. The mixture was used to transfection of the cancer cells. Predesigned *siRET* pools (No. 5979–1,2,3), *siYES1* pools (No. 7525–1,2,3), and negative control siRNA (#SN-1001) were purchased from Bioneer (Daejeon, South Korea). Predesigned si*NUAK1 (ARK5)* (#J-004931–10-0010) was purchased from Dharmacon (Lafayette, CO, USA).

2.10. Plasmid overexpression

The overexpression of *CCDC6-RET* was carried out using the same protocol as that for siRNA transfection, using Lipofectamine 2000 transfection reagents. *pEGFP-C1-CCDC6-RET* plasmid (#DU16863) was purchased from MRC PPU Reagents and Services (Dundee, UK).

2.11. Flank xenograft mouse model

Ba/F3 cells expressing CCDC6-RET (1×10^7 cells/100 μL of PBS) and HCC827 cells (1×10^7 cells/100 μL of PBS) were injected subcutaneously into the flanks of 6-week-old male BALB/c-nu mice. When tumor became palpable (approximately 150 mm^3), PLM-101 and vehicle were administered once a day for the indicated days through oral gavage (PO). Tumor volume and body weight were measured twice a week. Tumor volume was calculated using a caliper as followed formula: length x ($width^2$) x 0.5. All procedures were approved by the Institutional Animal Care and Use Committee of Seoul National University (Approval #SNU-190417-3, #SNU-211022-5). Mice were obtained from JA BIO (Suwon, South Korea) and maintained in the specific-pathogen-free facility of Seoul National University Institute of Laboratory Animal Resources (Seoul, South Korea).

2.12. Trans-well invasion assay

Cancer cells (3000 cells/well) were seeded in the IncuCyte Clearview 96-well plate for chemotaxis (#4582, Sartorius, Gottingen, Germany). To create a gradient of chemoattractant, 1 % FBS was added to the upper well, while 15 % FBS was added to the lower well. PLM-101 and vehicle were added to both the upper and lower wells at the indicated concentrations. The number of cells above and below was scanned and analyzed by IncuCyte Zoom/IncuCyte S3 Live Cell Analysis System (Sartorius).

2.13. Phalloidin (F-actin) staining: confocal microscopy and flow cytometry

Alexa Fluor 488 Phalloidin (#A12379, Invitrogen) was used to the stain F-actin in cancer cells, according to the instructions provided in the manual. The stained cells were detected for F-actin image and intensity using confocal microscopy (TCS SP8, Leica, wetzlar, Germany) and flow cytometry (Novocyte, Agilent), respectively.

2.14. Public data analysis

The data for GSE28248 were obtained from the NCBI (National Center for Biotechnology Information) database. This study aimed to analyze the expression of *YES1* gene in intratumor or peritumor regions of hepatocellular carcinoma patients with or without lymphatic metastases. The plots depicting the survival rates of lung cancer patients were acquired from GEPIA, which is a web server used for cancer and normal

gene expression profiling and interactive analyses. This study examined the overall survival of liver cancer and lung cancer patients based on their *YES1* gene expression levels.

2.15. Lung metastasis by tail vein injection

HCC827 cells were transfected with lentiviral particles of the CMV-Luciferase (firefly)-RFP gene (#LVP009, AMSBIO, Cambridge, MA, USA) to generate HCC827-luc-RFP cell line. HCC827-luc-RFP cells (2 $\times 10^5$) were suspended in 100 μL PBS and injected into the tail vein of 6-week-old male NOD/ShiLtJ-*Prkdc*^{em1AMC}*Il2rg*^{em1AMC} (NSGA) mice. PLM-101 was orally administered for five days before the injection of cells, and was continuously given orally every day throughout the experimental period. Bioluminescence intensity in the lung was detected every week using IVIS Spectrum In Vivo Imaging System (PerkinElmer). 150 mg/kg D-Luciferin Potassium Salt (#122799, PerkinElmer) was injected intraperitoneally into the mice 10 min before detection. All procedures were approved by the Institutional Animal Care and Use Committee of

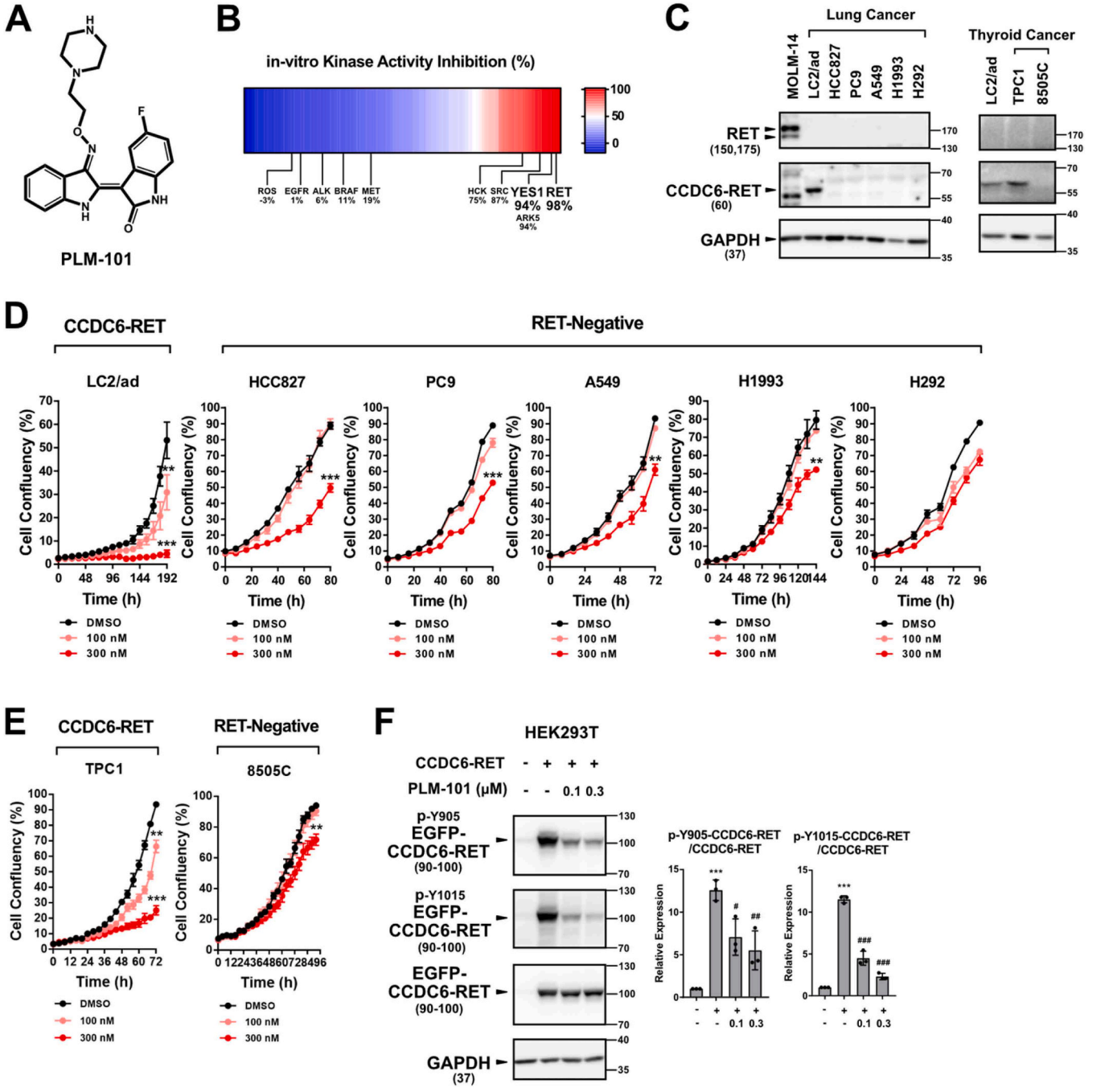

Fig. 1. Identification of anti-cancer active compound targeting CCDC6-RET. **(A)** The structure of the PLM-101. **(B)** *In vitro* kinase activity assay results using 100 nM PLM-101, a total of 96 kinases in library were evaluated. **(C)** The basal expression levels of RET and CCDC6-RET protein in lung and thyroid cancer cell lines. MOLM-14 acute myeloid leukemia cell line was used as a RET-wild type-positive cell line. **(D)** Anti-proliferative activities of PLM-101 against various lung cancer cell lines. **(E)** Anti-proliferative activities of PLM-101 against various thyroid cancer cell lines. **(F)** Inhibition of cellular CCDC6-RET activity by PLM-101 in CCDC6-RET overexpressing HEK293T cells. In Figure F, HEK293T cells were treated with PLM-101 for 3 h after the plasmid transfection. All data represent the mean ± SD. Statistical significance of the differences in Fig. 1 was determined by one-way ANOVA followed by the Tukey's test. *p < 0.05, * *p < 0.01, * **p < 0.001, significance compared to control group.

Seoul National University (Approval #SNU-210915–3-2, #SNU-221015–1-2). Mice were obtained from JA BIO (Suwon, South Korea) and maintained in the specific-pathogen-free facility of Seoul National University Institute of Laboratory Animal Resources (Seoul, South Korea).

2.16. Statistical analysis

Statistical significance was assessed using GraphPad Prism 7.0. One-way ANOVA followed by the Tukey's test or unpaired two-tailed Student t-test were used to analyze the significance between experimental groups. *P* values less than 0.05 were considered as significant differences. *P* value presented in this study follows the NEJM style; *p < 0.05, **p < 0.01, ***p < 0.001.

3. Results

3.1. Novel anti-cancer agent PLM-101 targets CCDC6-RET

Through an *in vitro* kinase activity assay on a library of 96 kinases, PLM-101 was identified as a potent inhibitor of RET activity (Fig. 1A, B). This compound exhibited low inhibitory activity against the ROS, EGFR, ALK, BRAF, and MET kinases, which are the primary targets for lung cancer treatment (Fig. 1B). Further *in vitro* kinase assays and Ba/F3 assays were conducted to evaluate the inhibitory activities of PLM-101 against clinically identified rearranged and mutant forms of RET. PLM-101 displayed strong inhibitory activities against CCDC6-RET (0.587 nM) and KIF5B-RET (0.385 nM), which are representative RET rearrangement proteins (Table 1). The compound also showed inhibitory activities against the V804M and V804L mutations, known as gatekeeper mutations associated with resistance to RET-targeting therapy (Table 1). We then assessed the protein expression of RET protein in various lung cancer and thyroid cancer cell lines. CCDC6-RET protein expression was detected in LC2/ad lung cancer cells and TPC1 thyroid cancer cells, while wild-type RET protein was not expressed in any of the lung cancer or thyroid cancer cell lines (Fig. 1C). To confirm the inhibitory effect of PLM-101 on cancer cell proliferation by targeting of the CCDC6-RET protein, each cell line was treated with vehicle or PLM-101, and their proliferations were evaluated. PLM-101 exhibited a strong inhibitory effect on cancer cell proliferation only in CCDC6-RET-expressing cancer cells, LC2/ad and TPC1 (Fig. 1D, E). The decreased phosphorylation of CCDC6-RET kinase confirmed that the activity of CCDC6-RET in cancer cells could be effectively suppressed by PLM-101 treatment (Fig. 1F).

3.2. PLM-101 treatment induces apoptosis and cell-cycle arrest in CCDC6-RET cancer cells

To assess the effect of PLM-101 on the colony-forming ability of cancer cells, cancer cell lines were seeded at low density on a 6-well plate and treated with the drug. Similar to the results shown in Fig. 1, PLM-101 demonstrated more potent inhibitory activity against colony formation in CCDC6-RET-expressing cancer cells compared to RET-negative lung cancer and thyroid cancer cell lines (Fig. 2A–D). Additionally, PLM-101 induced cell-cycle arrest and apoptosis, as analyzed by flow cytometry (Fig. 2E, F). Furthermore, increased cleavage of PARP and Caspase-3, representative markers of apoptosis, as well as reduced levels of Cyclin D1, Cyclin E, and Cyclin B1, indicative markers of cell-cycle arrest, were confirmed (Fig. 2G, H). These results indicate that PLM-101 effectively inhibits CCDC6-RET-expressing cancer cells by inducing apoptosis, cell-cycle arrest, and inhibiting colony formation.

Table 1
In vitro kinase activity assays and BaF3 proliferation assays for different RET kinase mutation or rearrangement forms.

RET inhibitor		PLM-101
RET Kinase Activity (IC_{50}, nM)	RET	0.849
	RET-M918T	0.838
	RET-KIF5B	0.385
	RET-CCDC6 (PTC1)	0.587
	RET-PRKAR1A (PTC2)	0.266
	RET-NCOA4 (PTC3)	3.69
BaF3-RET (GI_{50}, nM)	RET-CCDC6	25.9
	RET-CCDC6-V804M	3.4
	RET-CCDC6-V804L	190.2
	RET-KIF5B	75.2
	RET-KIF5B-V804L	55.3
	RET-KIF5B-V804M	53.7

3.3. Targeting of CCDC6-RET by PLM-101 blocks RAS/MAPK and PI3K/AKT pathways

To investigate the mechanism by which CCDC6-RET activates cancer cells, we overexpressed CCDC6-RET in HEK293T cells. Overexpression of CCDC6-RET increased the activities of components of the RAS pathway, including MEK, ERK, and p90RSK, as well as components of the PI3K pathway, such as AKT and p70S6K (Fig. 3A). Conversely, knockdown of CCDC6-RET by siRNA in LC2/ad and TPC1 cells inhibited the activation of the RAS and PI3K signaling pathways (Fig. 3B, C). These results serve to demonstrate that abnormal CCDC6-RET expression in cancer cells promotes proliferation through activation of the RAS/MAPK and PI3K/AKT pathways. To confirm whether PLM-101 could block the RAS and PI3K pathways activated by CCDC6-RET, CCDC6-RET-overexpressing HEK293T cells were treated with PLM-101. The downstream kinase activities of the RAS and PI3K pathways were effectively suppressed by PLM-101 (Fig. 3D). Similarly, PLM-101 blocked the activity of the RAS and PI3K pathways in CCDC6-RET-expressing LC2/ad and TPC1 cells (Fig. 3E, F). However, PLM-101 failed to block the activity of the RAS and PI3K pathways in HCC827, PC9, 8505 C cells, and the RET-negative cancer cell lines (Fig. 3G–I). Therefore, we concluded that potent inhibition of CCDC6-RET and its downstream signaling by PLM-101 mainly contribute to the anti-proliferative effects of PLM-101 in LC2/ad and TPC1 cancer cells.

3.4. Anti-cancer effect of PLM-101 on in vivo flank mouse tumor model

To assess the pre-clinical anti-cancer activity of PLM-101 against CCDC6-RET-expressing cancer cells, we implanted Ba/F3-CCDC6-RET cells into the flank of BALB/c nude mice and administered PLM-101 orally once a day (Fig. 4A). Neither LC2/ad nor TPC1 cells could be engrafted in either BALB/c nude mice or NOD/ShiLtJ-*Prkdc*^{em1AMC}*Il2rg*^{em1AMC} (NSGA) mice. Therefore, they were judged to be not applicable to *in vivo* pre-clinical experiments. Xenograft experiments demonstrated that oral administration of PLM-101 has anti-cancer effects on CCDC6-RET-positive tumor (Fig. 4B, C), and only slight changes in body weight were observed (Fig. 4D). Overall, these findings provide evidence that oral administration of PLM-101 suppresses the growth of primary cancers expressing CCDC6-RET.

3.5. Identification of lung cancer metastasis mechanism through the YES1-Cortactin-actin remodeling pathway

Metastasis, the spread of primary cancer to different parts of the body, is a major cause of cancer-related mortality [16,17]. Lung cancer, in particular, is notorious for its rapid metastatic potential [18]. Therefore, it is crucial to uncover the mechanisms underlying lung cancer metastasis and to develop effective targeting strategies. YES1, a target of PLM-101 (Fig. 1B), belongs to the SRC family kinases. Whereas other kinases in this family have been implicated in cancer growth and metastasis, the role of YES1 remains unstudied [32,33]. To investigate the involvement of YES1 in cancer cell metastasis, we compared its expression levels between metastatic and non-metastatic cancer tissues. Public data analysis (GSE28248) confirmed a significant increase in

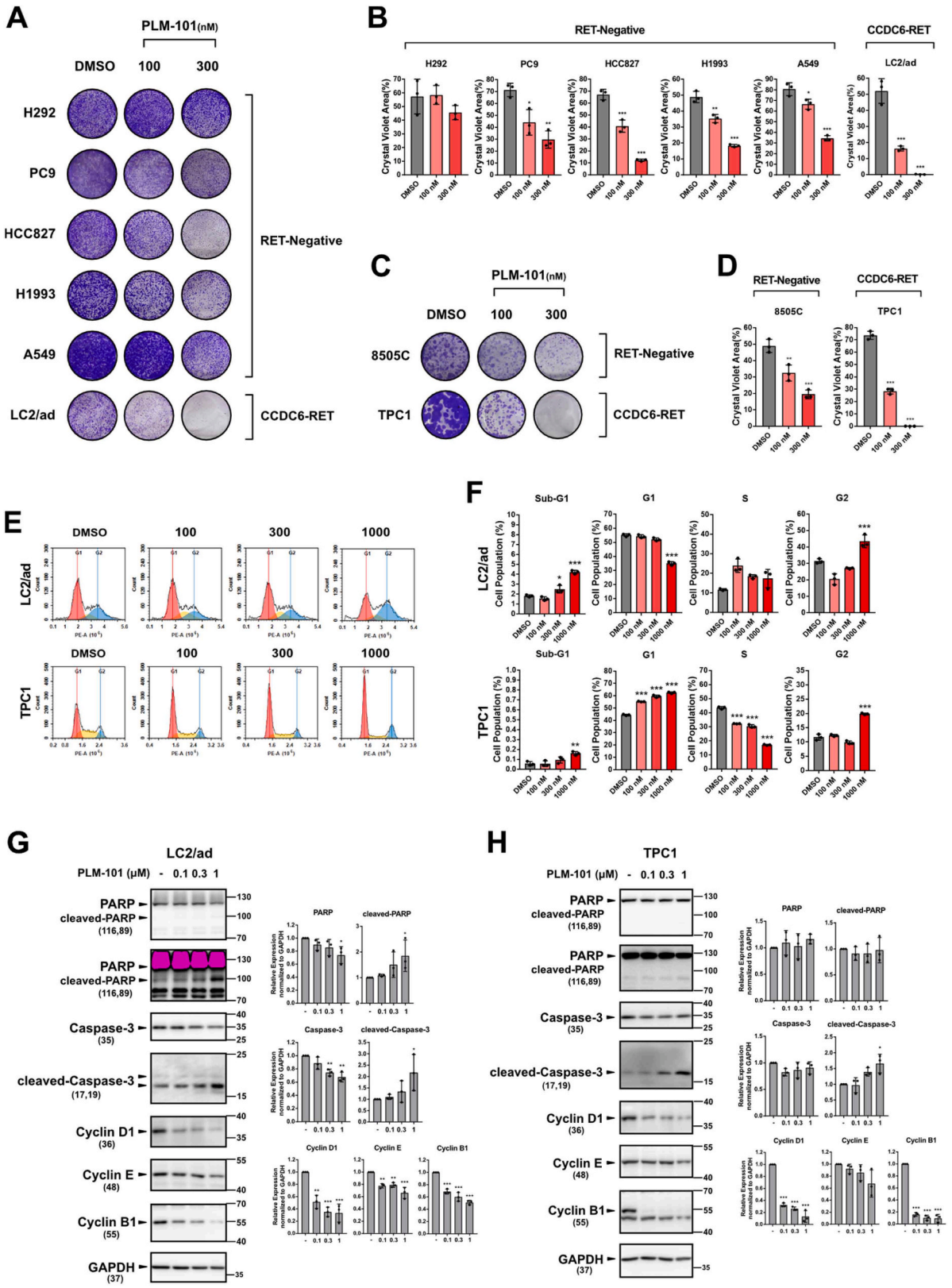

Fig. 2. Inhibition of colony formation and induction of apoptosis and cell cycle arrest by PLM-101.**(A)** Effects of PLM-101 on colony formation assays using various lung cancer cell lines. **(B)** Crystal violet positive area of Figure A. **(C)** Effects of PLM-101 on colony formation assay using two thyroid cancer cell lines. **(D)** Crystal violet positive area of Figure C. **(E)** Effect of PLM-101 on cell cycle. Flow cytometry analysis was performed after propidium iodide staining. **(F)** The calculation of the percentage in each cell cycle stage. **(G, H)** The protein expression changes in markers of apoptosis (cleaved-PARP, cleaved-caspase-3) and cell cycle (cyclin D1, E, B1) by PLM-101 treatment. In Figure E-H, PLM-101 was treated for 24 h at the indicated concentration. All data represent the mean ± SD. Statistical significance of the differences in Fig. 2 was determined by one-way ANOVA followed by the Tukey's test. *$p < 0.05$, **$p < 0.01$, ***$p < 0.001$, significance compared to control group.

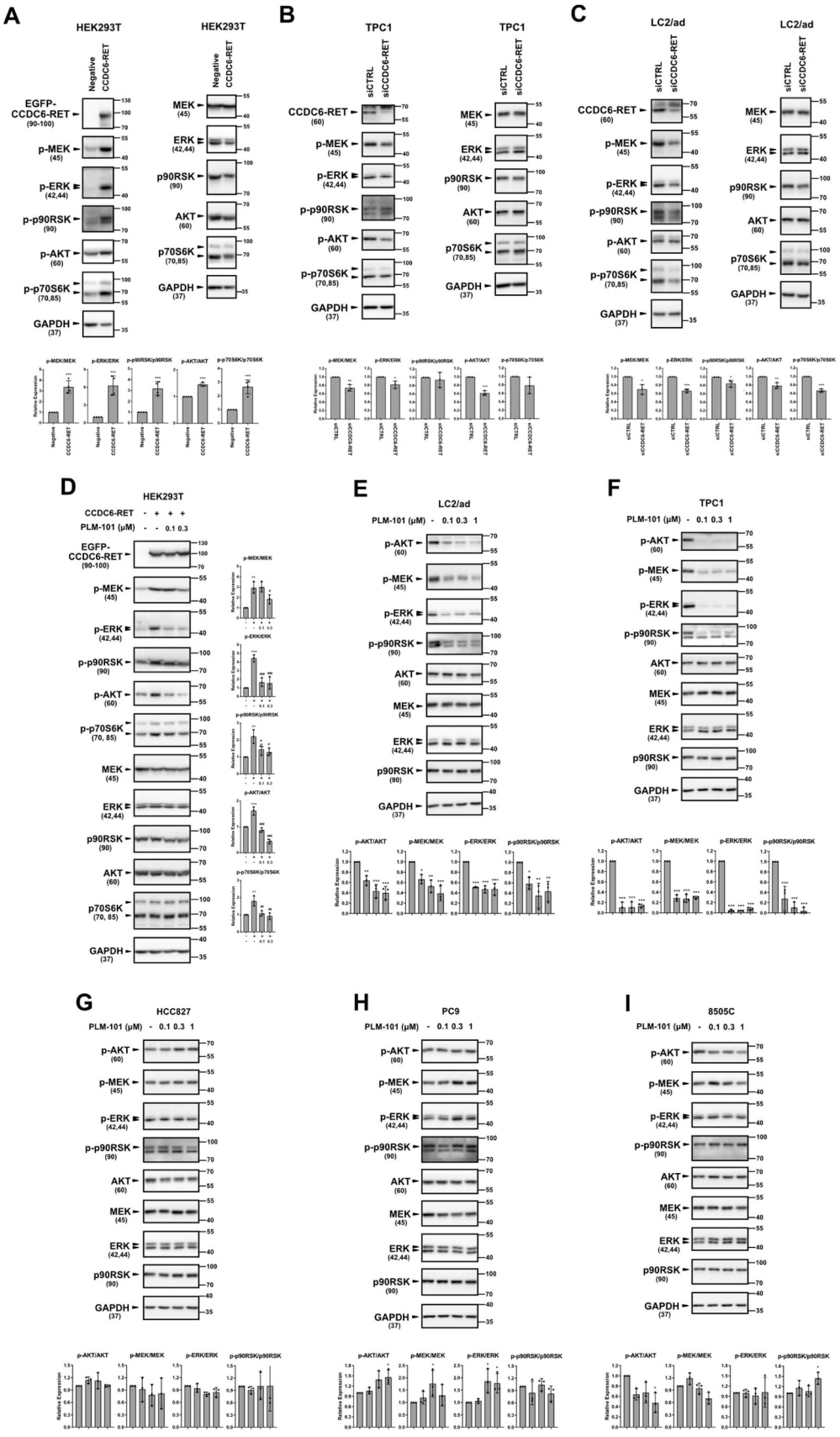

(caption on next page)

Fig. 3. PLM-101 exerts anti-cancer activity by inhibiting PI3K and RAS signaling pathways through targeting CCDC6-RET.**(A)** Activation of PI3K pathway (phospho-S473 AKT and phospho-T389 p70S6K) and RAS pathway (phospho-S217/S221 MEK, phospho-T202/Y204 ERK, and phospho-S380 p90RSK) by CCDC6-RET overexpression in HEK293T cells. **(B, C)** Inhibition of PI3K pathway and RAS pathway by knockdown of *CCDC6-RET* in CCDC6-RET-positive cell lines. **(D)** Inhibition of PI3K pathway (phospho-S473 AKT) and RAS pathway (phospho-S217/S221 MEK, phospho-T202/Y204 ERK, and phospho-S380 p90RSK) by PLM-101 in CCDC6-RET overexpressing HEK293T cells. **(E, F)** Inhibition of PI3K pathway and RAS pathway by PLM-101 in CCDC6-RET-positive cell lines, LC2/ad and TPC1. **(G-I)** Inhibition of PI3K and RAS pathways by PLM-101 in RET-negative cell lines, HCC827, PC9, and 8505 C. In all Figures, PLM-101 was treated for 3 h at the indicated concentration. All data represent the mean ± SD. Statistical significance of the differences in Fig. 3 was determined by one-way ANOVA followed by the Tukey's test. *p < 0.05, * *p < 0.01, * **p < 0.001, significance compared to control group.

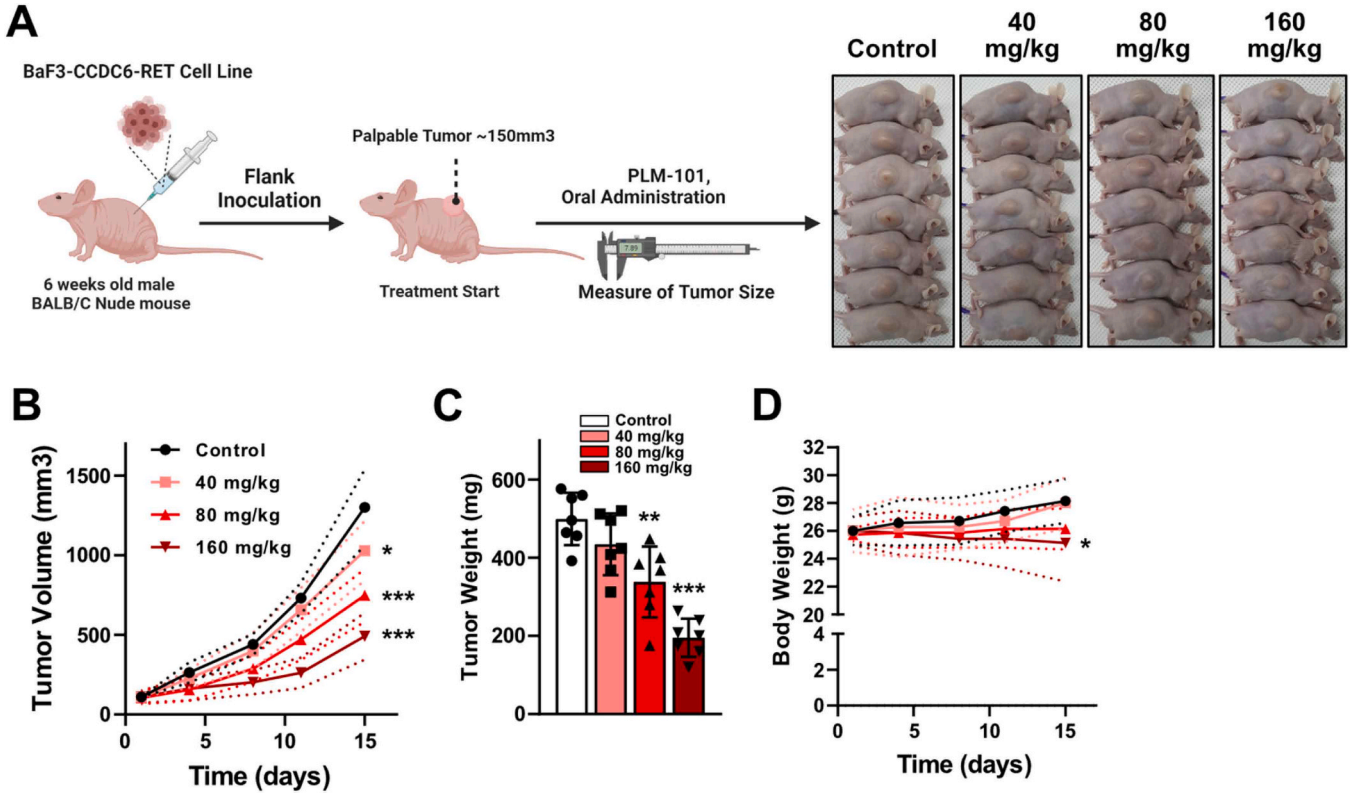

Fig. 4. *In vivo* anti-cancer effect of PLM-101 in Ba/F3-CCDC6-RET xenografts. (A) Schematic illustration of *in vivo* flank xenograft mouse model. CCDC6-RET expressing Ba/F3 cells were engrafted in the flanks of 6-week-old male BALB/c-nu mice. After the tumor volume reaches ~150 mm3, PLM-101 was administered orally once a day. Tumor volume and body weight were measured twice a week. (B, C) Anti-tumor efficacy of PLM-101 in Ba/F3-CCDC6-RET flank allograft model. N = 7. (D) Changes in body weight during PLM-101 treatment. N = 7. All data represent the mean ± SD. Statistical significance of the differences in Fig. 4 was determined by one-way ANOVA followed by the Tukey's test. *p < 0.05, **p < 0.01, ***p < 0.001, significance compared to control group.

YES1 expression in cancer tissues that had metastasized from hepatocellular carcinoma to lymph nodes (Fig. 5A). Moreover, patients with high YES1 expression in liver or lung cancer exhibited decreased survival rates, with hazard ratios (HR) of 1.2 and 1.3, respectively (Fig. 5B). Previous studies have shown that SRC regulates cancer cell migration and metastasis by modulating the activity of Cortactin, an actin polymerization protein [37,41]. First, we assessed the *in vitro* cell migration ability and YES1 expression levels in various lung cancer cells. Because LC2/ad cells expressing CCDC6-RET lacked migrating ability, HCC827 and PC9 cells, which possess both metastatic potential and high levels of YES1, were employed (Fig. S1A, S1B). To investigate whether YES1 also regulates Cortactin activity, YES1-specific siRNAs were introduced into both cell types. Knockdown of YES1 resulted in inhibition of Cortactin activity (Fig. 5C, D) and reduced cancer cell migration (Fig. 5E, F), implying that YES1 can regulate cancer cell migration by activation of Cortactin. Building upon a previous study that revealed that KIF5B-RET regulates cancer cell invadopodia via SRC activation [42], we examined whether CCDC6-RET can modulate YES1 activity. Overexpression of CCDC6-RET in HEK293T cells increased phosphorylation of YES1 and Cortactin (Fig. 5G), suggesting that CCDC6-RET may regulate cancer metastasis by influencing the YES1-Cortactin pathway.

3.6. YES1-targeting therapy inhibits metastasis of lung cancer cells by suppressing YES1-Cortactin-actin remodeling pathway

To investigate whether YES1-targeting therapies can suppress Cortactin activity, we used Dasatinib, an FDA-approved anti-cancer agent that non-selectively inhibits YES1 and other SRC family kinases [39], as well as PLM-101. Indeed, YES1-targeting agents, PLM-101 and Dasatinib suppressed Cortactin activity by inhibiting YES1 (Fig. 6A–D), and also hindered cancer cell migration at concentrations lower than those causing cytostatic inhibition (Fig. 6E–H). To confirm that the inhibition of cancer cell migration by PLM-101 occurred through the effects on actin polymerization, the F-actin intensity and morphology were analyzed. The findings showed that PLM-101 treatment led to decreased F-actin intensity and morphology disruption (Fig. 6I, J). We further examined whether YES1 inhibition affects other mechanism(s) involved in metastasis, such as changes in epithelial-mesenchymal transition (EMT) and Matrix Metalloproteinases (MMP) markers [40]. Neither YES1-targeting therapy nor YES1 knockdown induced changes in EMT-related or MMP proteins (Fig. S2A-S2H). Collectively, these results indicate that PLM-101 inhibits cancer cell migration by targeting YES1 and subsequently suppressing the Cortactin-actin remodeling pathway.

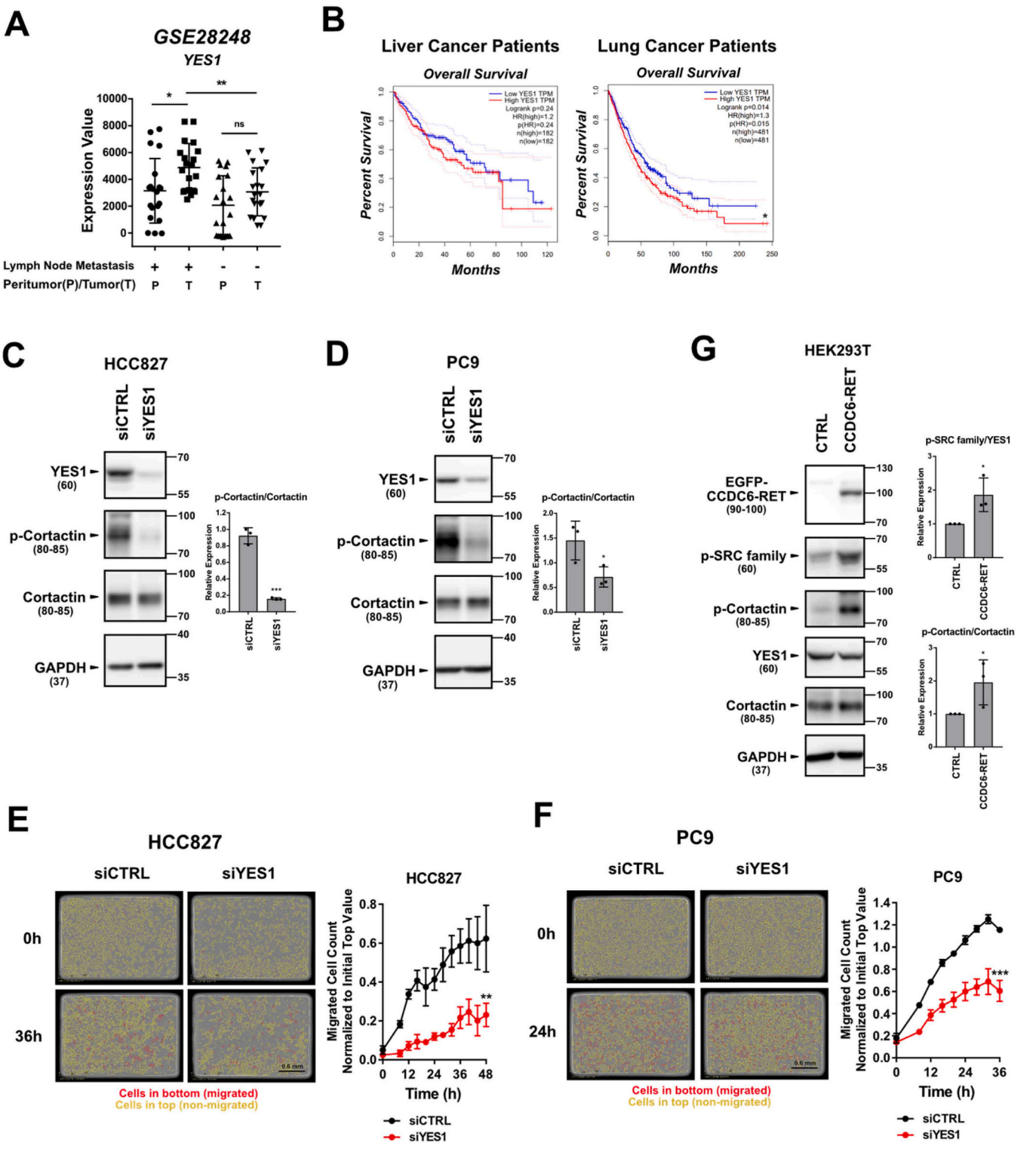

Fig. 5. Metastasis and cancer cell migration through YES1-Cortactin signaling **(A)** Comparison of *YES1* mRNA expression levels in hepatocellular carcinoma patients with and without lymph node metastasis. Public data were obtained from the NCBI database (GSE28248). **(B)** Comparison of survival rate based on *YES1* expression in liver and lung cancer patients. Public data was obtained from the GEPIA. **(C, D)** Changes in Cortactin activity (phospho-Y421 Cortactin) by *YES1* specific knockdown in HCC827 and PC9 cells. **(E, F)** Anti-migration activity by *YES1* specific knockdown. **(G)** Changes in YES1 and Cortactin activity by CCDC6-RET overexpression. All data represent the mean ± SD. Statistical significance of the differences in Fig. 5A was determined by one-way ANOVA followed by the Tukey's test. Statistical significance of the differences in Fig. E and F were determined by unpaired two-tailed Student t-test. *$p < 0.05$, **$p < 0.01$, ***$p < 0.001$, significance compared to control group.

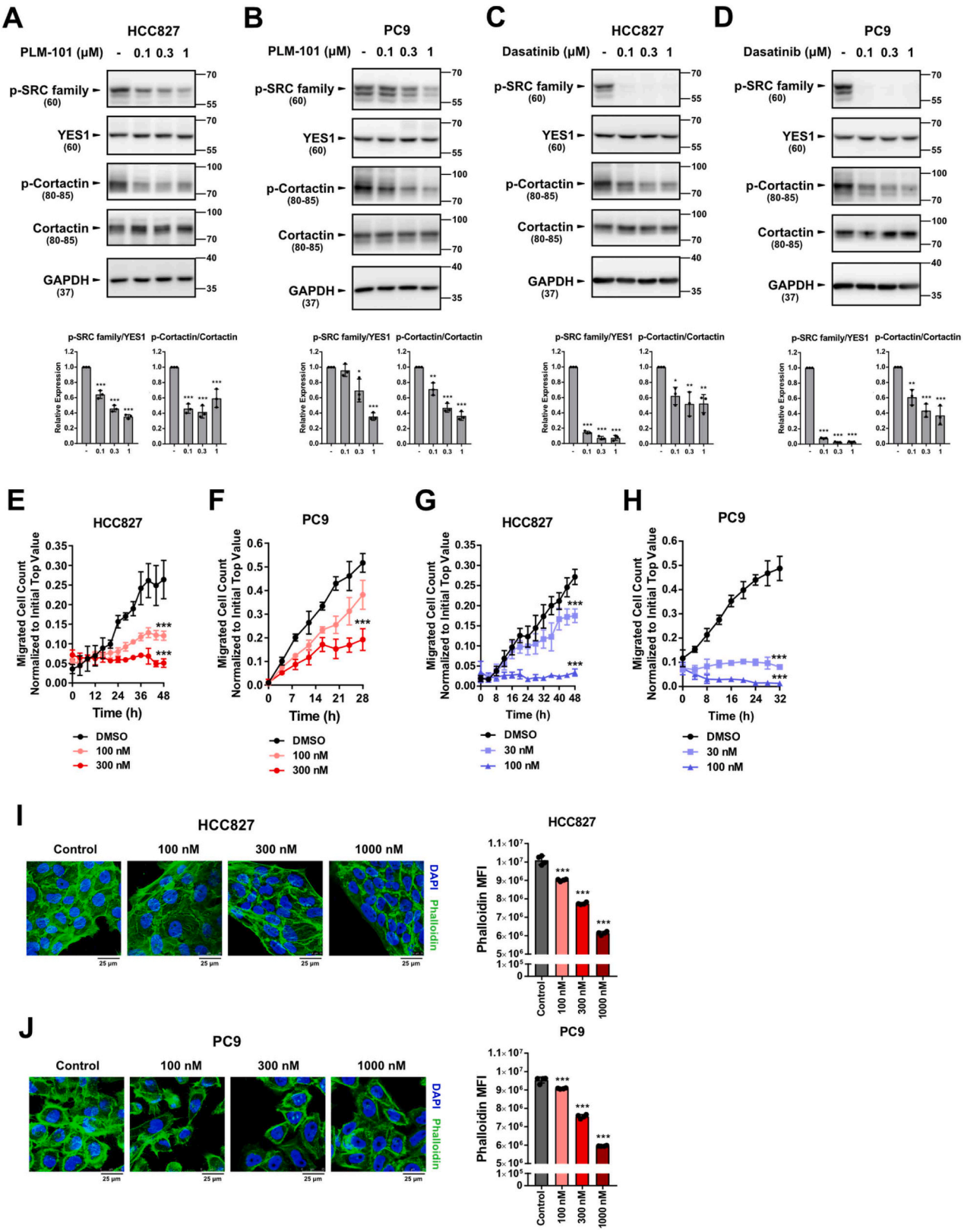

Fig. 6. YES1-targeting agents inhibit migration of cancer cells by inhibiting Cortactin-actin remodeling activity (A, B) Inhibition of YES1 and Cortactin activities by PLM-101. **(C, D)** Inhibition of YES1 and Cortactin activity by Dasatinib. In Figure A-D, YES1-targeting agents were treated for 3 h at the indicated concentration. **(E, F)** Inhibition of cancer cell migration by PLM-101. **(G, H)** Inhibition of cancer cell migration by Dasatinib. **(I, J)** Confocal microscopy images. Green: phalloidin (F-actin). Blue: DAPI (nucleus). Phalloidin (F-actin) intensity was quantified using flow cytometry. In Figure I, J, PLM-101 was treated for 24 h at the indicated concentration. All data represent the mean ± SD. Statistical significance of the differences in Fig. 6 was determined by one-way ANOVA followed by the Tukey's test. *p < 0.05, **p < 0.01, ***p < 0.001, significance compared to control group.

Despite CCDC6-RET-expressing LC2/ad cells lack of migrating ability, Cortactin phosphorylation was inhibited by YES1-targeting agent or YES1-specific knockdown (Fig. S3A, S3B).

3.7. Anti-metastatic effect of PLM-101 on in vivo IV-lung metastasis model

To validate the efficacy of PLM-101 in a pre-clinical metastasis model, an IV-lung metastasis model was employed. In this model, cancer cells injected into the tail vein metastasize from the bloodstream to the lung through extravasation, a key stage of metastasis [41]. Because CCDC6-RET-expressing LC2/ad and TPC1 cells do not show *in vitro* migration ability and cannot be implanted into even immune-deficient mice, the HCC827 cell line, metastatic lung cancer cells expressing YES1, was used. NSGA mice were orally pretreated with vehicle or PLM-101 (40 mg/kg) for five days, followed by injection of luciferase-overexpressing metastatic lung cancer cells (HCC827-luc-RFP) via the tail vein (Fig. 7A). Throughout the

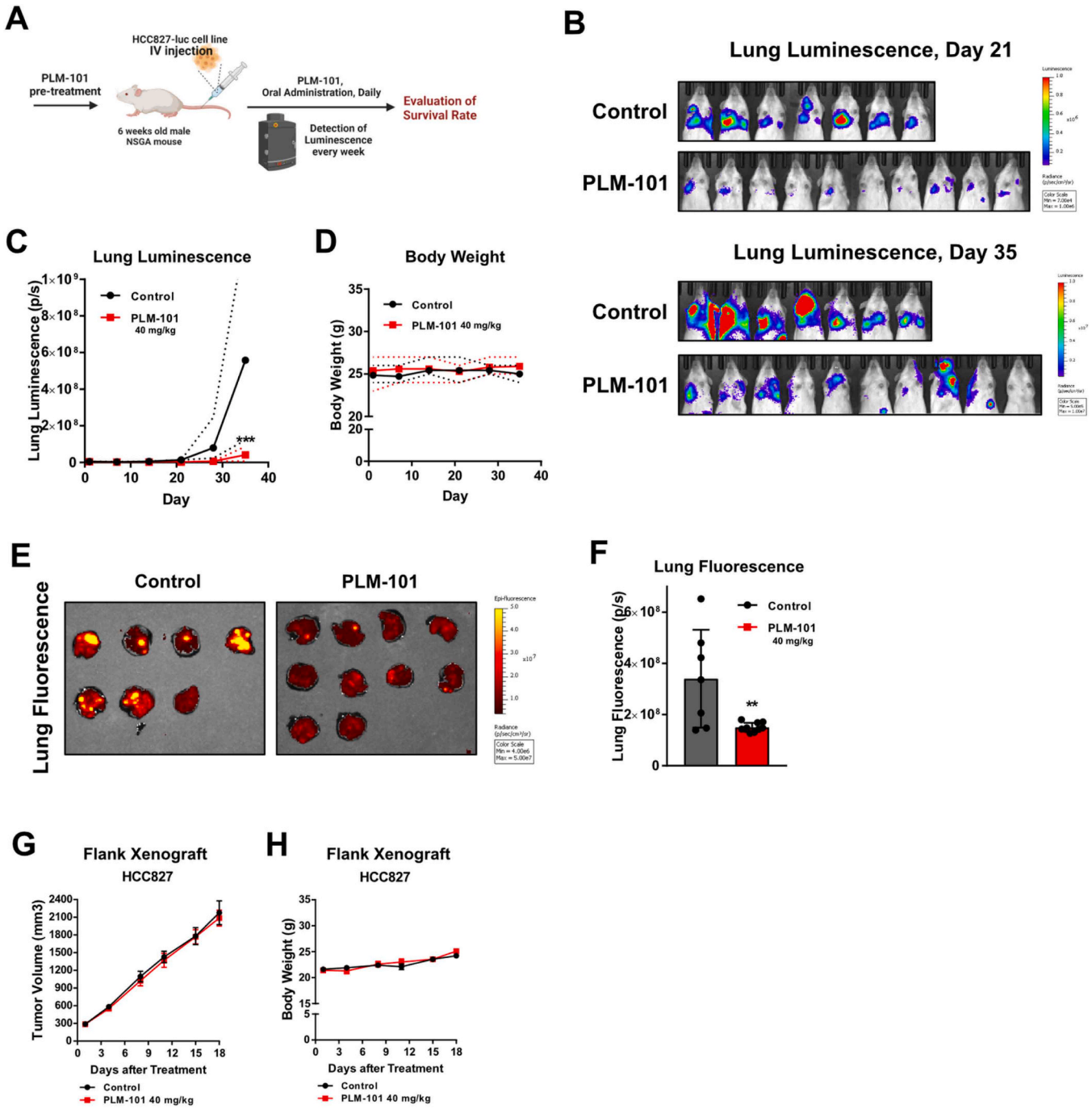

Fig. 7. Anti-metastatic effect of PLM-101 in IV-lung metastasis model **(A)** Schematic illustration of IV-lung metastasis model. 6-week-old male NSGA mice were used. After pretreatment with PLM-101 for 5 days, HCC827-luc-RFP cells were injected into tail vein. 40 mg/kg PLM-101 was administered orally in a daily basis and bioluminescence was measured once a week. **(B)** The picture of bioluminescence, **(C)** lung luminescence (photons/sec), **(D)** body weight, in IV-lung metastasis model. N = 7. **(E)** The RFP-fluorescence in lung, and **(F)** intensity of RFP-fluorescence on day 35. **(G, H)** Anti-cancer activity of PLM-101 in HCC827 flank xenograft model. N = 6. All data represent the mean ± SD. Statistical significance of the differences in Fig. 7 was determined by one-way ANOVA followed by the Tukey's test. *p < 0.05, **p < 0.01, ***p < 0.001, significance compared to control group.

experiment, PLM-101 was administered orally to the mice daily, and the bioluminescence intensity was measured weekly. Bioluminescence imaging revealed that PLM-101 reduced the number of cancer cells metastasizing to the lungs of the mice (Fig. 7B, C), while the body weights of the mice remained unchanged during the experiment (Fig. 7D). On day 35, the mice were sacrificed, and their lungs were isolated to detect the RFP-fluorescence of the metastasized cancer cells. Consistent with the bioluminescence results, the group administered with PLM-101 showed decreased RFP-fluorescence in the lungs (Fig. 7E, F). However, in contrast to the IV-lung metastasis model, the administration of PLM-101 did not result in any reduction in primary tumor volume in the flank xenograft mouse model using HCC827 cells (Fig. 7G, H). In summary, these results confirm that PLM-101 can diminish metastasis of cancer cells in mice, presumably by inhibiting the YES1-Cortactin-actin remodeling pathway.

4. Discussion

Currently, only two RET-targeting agents, Pralsetinib and Selpercatinib, have been approved by the U.S. FDA and are being used for the treatment of RET fusion-positive solid tumors [11]. However, these RET-targeting agents have limited efficacy, with objective response rates (ORRs) of 64 % and 57 % in the Selpercatinib [42] and Pralsetinib [43] treatment groups, respectively. Therefore, development of new RET-targeting drugs with improved efficacy is a clinical task of great urgency. In this study, we scrutinized a new RET-targeting compound, PLM-101. PLM-101 efficiently suppressed the activities of CCDC6-RET and KIF5B-RET, the major forms of RET rearrangement. Additionally, PLM-101 exhibited potent inhibitory activity against their gatekeeper mutations, V804M and V804L (Table 1). Notably, PLM-101 demonstrated stronger anti-proliferative (Fig. 1D, E) and anti-colony formation effects (Fig. 2B, C) in CCDC6-RET-expressing cancer cells, LC2/ad and TPC1, relative to RET-negative cancer cells. Although we did not have access to cancer cells expressing KIF5B-RET for experimentation, it can be predicted that PLM-101 would exhibit similar anti-cancer effects against them. Efficacy experiments with a flank xenograft model further revealed that oral administration of PLM-101 effectively reduced the volume of CCDC6-RET-expressing primary tumors (Fig. 4). Collectively, these data suggest PLM-101′s potential for treatment of RET rearrangement cancer. A higher concentration range of PLM-101 (300 nM) evoked marginal anti-proliferation effects in all of the tested lung cancer cell lines (Fig. 1D). PLM-101 blocked activation of mTOR complex 1, as evidenced by the inhibition of phospho-S2448 mTOR and phospho-T389 p70S6K, irrespective of CCDC6-RET expression (Fig. S4A-S4F). This effect can be attributed to the multi-target kinase inhibitory property of PLM-101 in cases where one of the minor targets, ARK5, being involved in regulation between AKT and mTOR complex 1. This was confirmed through an ARK5-specific knockdown experiment (Fig. S4G). Thus, the marginal suppression of proliferation in RET-negative cancer cells by PLM-101 at concentrations above 300 nM may result from inhibition of ARK5 activity (Fig. 1D, E).

Lung cancer not only is a dangerous primary tumor but also has a high potential for metastasis, characterized by rapid spread to various organs [17,18]. Metastatic secondary tumors significantly affect the survival of cancer patients [17]. Despite the importance of preventing metastasis, its underlying mechanism is not yet fully understood, and indeed, has not been effectively targeted [24]. Therefore, it is important to identify and target the metastasis mechanism of lung cancer. One of the mechanisms of cancer cell metastasis is the formation of protrusive structures, such as filopodia, lamellipodia, and invadopodia, through actin polymerization [26,44,45]. In this study, we confirmed that YES1, one of the SRC family kinases, regulates cancer cell metastasis by controlling actin polymerization through the regulation of Cortactin activity. Specific knockdown of YES1 suppressed the metastatic ability of lung cancer cells by inhibiting Cortactin activity (Fig. 5C–F). Moreover, treatment with YES1-targeting agents, PLM-101 and Dasatinib, showed similar outcomes (Fig. 6A–H). YES1-specific knockdown and targeted therapy for YES1 did not affect any of the other mechanisms involved in metastasis, such as EMT and MMP (Fig. S3). Furthermore, oral administration of PLM-101 effectively inhibited the metastasis of cancer cells in an *in vivo* IV-lung metastasis mouse model (Fig. 7). Based on these findings, we propose PLM-101 as a new YES1-targeting agent that can effectively prevent cancer cell metastasis by inhibiting the YES1-Cortactin-actin remodeling pathway.

Clinical findings have shown that metastasis occurs more frequently in lung cancer with RET rearrangement [23]. Additionally, a recent study revealed that KIF5B-RET regulates invadopodia by regulating SRC activity [37]. Therefore, we tested the possibility that RET rearrangement contributes to lung cancer metastasis through SRC family kinases activity. Indeed, overexpression of CCDC6-RET in HEK293T cells increased the activity of the SRC family kinases and Cortactin (Fig. 5G). Furthermore, we confirmed that RET-specific knockdown suppressed SRC family kinases and Cortactin activity in CCDC6-RET-expressing LC2/ad cells (Fig. S3A). Unfortunately, additional research on the role of the CCDC6-RET-YES1-Cortactin-actin remodeling pathway on cancer metastasis could not be performed, due to the unavailability of RET-expressing cancer cell lines with metastatic potential. More studies are needed to elucidate whether the regulation of metastasis through the CCDC6-RET-YES1-Cortactin pathway is related to the high metastasis rates observed in RET rearrangement lung cancer patients.

Interestingly, RET-positive NSCLC appears to be 'cold' tumors with low PD-L1 expression [46]. Patients with RET-abnormal cancers treated with immune checkpoint inhibitors (ICI) have shown a shorter median time to progression compared with those receiving non-ICI treatment regimens [46]. Therefore, developing strategies to enhance the efficacy of immune-oncological agents for lung cancer patients with RET abnormalities is crucial. Recent studies have found that inhibitors of SRC family kinases enhance the responsiveness of cancer cells to immunotherapeutic agents [47–49]. Also, it has been demonstrated that concurrent administration of PD-1 antibody with the SRC family kinase inhibitor Dasatinib can trigger a potent immune response against cancer [47], and that co-treatment of PD-1 antibody with hematopoietic cell kinase (HCK) inhibitor RK20449 represents improved anti-tumor activity [48]. Clearly, investigating the underlying mechanism by which SRC family kinases, specifically YES1, enhance patient responsiveness to immunotherapy is necessary. This could pave the way for development of RET/YES1 or RET/SRC family kinases dual-target inhibitors, which could serve as the basis of a promising therapeutic strategy for treating lung cancer with RET abnormalities.

In conclusion, this study introduced a novel RET/YES1 dual-targeting agent, PLM-101, that effectively inhibits both primary tumors through its action on RET and secondary tumors through its action on YES1.

CRediT authorship contribution statement

Shim Wan Seob: Investigation. **Lee Young Joo:** Investigation. **Oh Su-jin:** Investigation. **Lee Jae-sun:** Investigation. **Kim Myung Jun:** Investigation. **Park Miso:** Investigation. **Park Jaewoo:** Investigation. **Kang Keon Wook:** Writing – review & editing, Supervision, Resources, Project administration, Funding acquisition, Conceptualization. **Choi Munkyung:** Investigation. **Kim Yong-Chul:** Supervision, Resources, Funding acquisition. **Choi Yong June:** Writing – review & editing, Writing – original draft, Visualization, Validation, Methodology, Investigation, Formal analysis, Conceptualization. **Kim Myung Jin:** Supervision, Resources. **Kim Ji Won:** Investigation.

Declaration of Competing Interest

JS Lee, SJ Oh, MJ Kim and YC Kim are working at PeLeMed.

Data Availability

Data will be made available on request.

Acknowledgements

This research was supported by the Technological Innovation R&D Program (S3029658) funded by the Ministry of SMEs and Startups (MSS, Korea) and the National Research Foundation of Korea (NRF) grant (2021R1A2C2093196) funded by the Korea government. All graphical figures were created using BioRender.com (BioRender, Toronto, Canada).

Appendix A. Supporting information

Supplementary data associated with this article can be found in the online version at doi:10.1016/j.biopha.2024.116124.

References

[1] C.S. Dela Cruz, L.T. Tanoue, R.A. Matthay, Lung cancer: epidemiology, etiology, and prevention, Clin. Chest Med. 32 (4) (2011) 605–644.
[2] A.J. Alberg, J.G. Ford, J.M. Samet, Epidemiology of lung cancer: ACCP evidence-based clinical practice guidelines (2nd edition), Chest 132 (3 Suppl) (2007) 29s–55s.
[3] F.R. Hirsch, et al., Lung cancer: current therapies and new targeted treatments, Lancet 389 (10066) (2017) 299–311.
[4] CO, C., Facts & Figures 2015–2016. 2015.
[5] L.A. Torre, R.L. Siegel, A. Jemal, Lung cancer statistics, in: A. Ahmad, S. Gadgeel (Eds.), Lung Cancer and Personalized Medicine: Current Knowledge and Therapies, Springer International Publishing, Cham, 2016, pp. 1–19.
[6] M. Wang, R.S. Herbst, C. Boshoff, Toward personalized treatment approaches for non-small-cell lung cancer, Nat. Med. 27 (8) (2021) 1345–1356.
[7] Kris, M., et al., Identification of driver mutations in tumor specimens from 1,000 patients with lung adenocarcinoma: The NCI's Lung Cancer Mutation Consortium (LCMC). Journal of Clinical Oncology, 2011.
[8] W. Pao, N. Girard, New driver mutations in non-small-cell lung cancer, Lancet Oncol. 12 (2) (2011) 175–180.
[9] A.C. Tan, D.S.W. Tan, Targeted therapies for lung cancer patients with oncogenic driver molecular alterations, J. Clin. Oncol. 40 (6) (2022) 611–625.
[10] Heist, R.S. and J.A. Engelman, SnapShot: Non-Small Cell Lung Cancer. Cancer Cell, 2012. 21(3): p. 448–448.e2.
[11] K.Z. Thein, et al., Precision therapy for RET-altered cancers with RET inhibitors, Trends Cancer 7 (12) (2021) 1074–1088.
[12] E. Arighi, M.G. Borrello, H. Sariola, RET tyrosine kinase signaling in development and cancer, Cytokine Growth Factor Rev. 16 (4-5) (2005) 441–467.
[13] G. Bronte, et al., Targeting RET-rearranged non-small-cell lung cancer: future prospects, Lung Cancer: Targets Ther. 10 (2019) 27–36.
[14] D. König, S. Savic Prince, S.I. Rothschild, Targeted therapy in advanced and metastatic non-small cell lung cancer. An update on treatment of the most important actionable oncogenic driver alterations, Cancers (Basel) 13 (4) (2021).
[15] M.J. Nokin, et al., Targeting infrequent driver alterations in non-small cell lung cancer, Trends Cancer 7 (5) (2021) 410–429.
[16] M. Riihimäki, et al., Metastatic sites and survival in lung cancer, Lung Cancer 86 (1) (2014) 78–84.
[17] H.H. Popper, Progression and metastasis of lung cancer, Cancer Metastas-.-. Rev. 35 (2016) 75–91.
[18] D.X. Nguyen, et al., WNT/TCF signaling through LEF1 and HOXB9 mediates lung adenocarcinoma metastasis, Cell 138 (1) (2009) 51–62.
[19] S.A. Hussain, D. Manogna, J. Shapiro, Metastatic lung adenocarcinoma with occult involvement of gluteal muscles as the sole site of distant metastases, Cureus 12 (8) (2020) e9826.
[20] F.-Y. Niu, et al., Distribution and prognosis of uncommon metastases from non-small cell lung cancer, BMC Cancer 16 (1) (2016) 149.
[21] T. Zhu, et al., Mechanisms and future of non-small cell lung cancer metastasis, Front. Oncol. 10 (2020).
[22] J. Li, et al., Prognostic value of site-specific metastases in lung cancer: a population based study, J. Cancer 10 (14) (2019) 3079–3086.
[23] A. Drilon, et al., Frequency of brain metastases and multikinase inhibitor outcomes in patients with RET-rearranged lung cancers, J. Thorac. Oncol. 13 (10) (2018) 1595–1601.
[24] J. Ko, M.M. Winslow, J. Sage, Mechanisms of small cell lung cancer metastasis, EMBO Mol. Med. 13 (1) (2021) e13122.
[25] H.K. Park, et al., Patterns of extrathoracic metastasis in lung cancer patients, Curr. Oncol. 29 (11) (2022) 8794–8801.
[26] R. Buccione, G. Caldieri, I. Ayala, Invadopodia: specialized tumor cell structures for the focal degradation of the extracellular matrix, Cancer Metastas Rev. 28 (1-2) (2009) 137–149.
[27] A.J. Ridley, Life at the leading edge, Cell 145 (7) (2011) 1012–1022.
[28] H.S. Leong, et al., Invadopodia are required for cancer cell extravasation and are a therapeutic target for metastasis, Cell Rep. 8 (5) (2014) 1558–1570.
[29] H. Yamaguchi, J. Condeelis, Regulation of the actin cytoskeleton in cancer cell migration and invasion, Biochim. Biophys. Acta 1773 (5) (2007) 642–652.
[30] H. Yamaguchi, J. Condeelis, Regulation of the actin cytoskeleton in cancer cell migration and invasion, Biochim. et. Biophys. Acta (BBA) - Mol. Cell Res. 1773 (5) (2007) 642–652.
[31] Y.A. Senis, A. Mazharian, J. Mori, Src family kinases: at the forefront of platelet activation, Blood J. Am. Soc. Hematol. 124 (13) (2014) 2013–2024.
[32] M.A. Ortiz, et al., Src family kinases, adaptor proteins and the actin cytoskeleton in epithelial-to-mesenchymal transition, Cell Commun. Signal. 19 (1) (2021) 67.
[33] Summy, J.M. and G.E. Gallick, Src family kinases in tumor progression and metastasis. Cancer Metastasis Rev, 2003. 22(4): p. 337–358.
[34] G. Bahlakeh, et al., Current knowledge and challenges associated with targeted delivery of neurotrophic factors into the central nervous system: focus on available approaches, Cell Biosci. 11 (1) (2021) 181.
[35] A. Hammer, S. Laghate, M. Diakonova, Src tyrosyl phosphorylates cortactin in response to prolactin, Biochem. Biophys. Res. Commun. 463 (4) (2015) 644–649.
[36] Y. He, et al., Src and cortactin promote lamellipodia protrusion and filopodia formation and stability in growth cones, Mol. Biol. Cell 26 (18) (2015) 3229–3244.
[37] T.K. Das, R.L. Cagan, KIF5B-RET oncoprotein signals through a multi-kinase signaling hub, Cell Rep. 20 (10) (2017) 2368–2383.
[38] H.J. Lee, et al., Characterization of LDD-2633 as a novel RET kinase inhibitor with anti-tumor effects in thyroid cancer, Pharm. (Basel) 14 (1) (2021).
[39] J. Araujo, C. Logothetis, Dasatinib: a potent SRC inhibitor in clinical development for the treatment of solid tumors, Cancer Treat. Rev. 36 (6) (2010) 492–500.
[40] A. Dongre, R.A. Weinberg, New insights into the mechanisms of epithelial–mesenchymal transition and implications for cancer, Nat. Rev. Mol. Cell Biol. 20 (2) (2019) 69–84.
[41] K.A. Thies, et al., Pathological analysis of lung metastasis following lateral tail-vein injection of tumor cells, J. Vis. Exp. (159) (2020).
[42] A. Drilon, et al., Efficacy of selpercatinib in RET fusion–positive non–small-cell lung cancer, N. Engl. J. Med. 383 (9) (2020) 813–824.
[43] V. Subbiah, et al., Pan-cancer efficacy of pralsetinib in patients with RET fusion–positive solid tumors from the phase 1/2 ARROW trial, Nat. Med. 28 (8) (2022) 1640–1645.
[44] G. Jacquemet, H. Hamidi, J. Ivaska, Filopodia in cell adhesion, 3D migration and cancer cell invasion, Curr. Opin. Cell Biol. 36 (2015) 23–31.
[45] C. Albiges-Rizo, et al., Actin machinery and mechanosensitivity in invadopodia, podosomes and focal adhesions, J. Cell Sci. 122 (17) (2009) 3037–3049.
[46] A. Hegde, et al., Responsiveness to immune checkpoint inhibitors versus other systemic therapies in RET-aberrant malignancies, ESMO Open 5 (5) (2020) e000799.
[47] E. Redin, et al., SRC family kinase (SFK) inhibitor dasatinib improves the antitumor activity of anti-PD-1 in NSCLC models by inhibiting Treg cell conversion and proliferation, J. Immunother. Cancer 9 (3) (2021).
[48] A.R. Poh, et al., Therapeutic inhibition of the SRC-kinase HCK facilitates T cell tumor infiltration and improves response to immunotherapy, Sci. Adv. 8 (25) (2022) eabl7882.
[49] G.T. Yu, et al., Inhibition of SRC family kinases facilitates anti-CTLA4 immunotherapy in head and neck squamous cell carcinoma, Cell Mol. Life Sci. 75 (22) (2018) 4223–4234.